JOURNAL OF OPTOELECTRONICS AND ADVANCED MATERIALS Vol. 26, No. 9-10, September - October 2024, p. 362 - 367

Thermal lens effect induced by laser beam in tetracarbonyl(2,2′-bipyridyl)chromium(0) complex

M. D. ZIDAN[1,*], M. M. AL-KTAIFANI[2], A. ALLAHHAM[1]
[1]*Department of Physics, Atomic Energy Commission, P. O. Box 6091, Damascus, Syria*
[2]*Department of Radioisotopes, Atomic Energy Commission, P. O. Box 6091, Damascus, Syria*

The thermal lens effect of Tetracarbonyl(2,2'-bipyridyl)chromium(0) complex (TCPC) solution was investigated using the mode-match dual beam z-scan technique. The thermal lens (TL) parameters of the TCPC solutions, such as: the convective velocity, thermal diffusivity, thermo-optic coefficient, on-axis phase shift, thermal diffusion time and Peclet number, were extracted using thermal lens theoretical model. It was found that with the increasing input pump laser powers, the thermal diffusion time and Peclet number decreased, while the on-axis phase shift increased as a result of the laser powers increase. As two wavelengths laser, λ_e=532 nm and λ_e=635 nm were used for excitation powers, the new results have shown how the wavelength effects molecular heat convection in the (TCPC) solution.

(Received May 15, 2024; accepted October 7, 2024)

Keywords: Thermal lens effect, Tetracarbonyl(2,2′-bipyridyl)chromium(0) complex, Thermo-optic coefficient, Peclet number, Nonlinear optical properties, Dual-beam z-scan technique

1. Introduction

Organometallic complexes (OMC) are very attractive molecular systems for fundamental linear and nonlinear optical studies. The size of the central metal and its position relative to the organic ligand are very important for their nonlinear optical properties [1-3]. The electrons of ***d*** orbital of the transition metal atoms usually have the appropriate energy and symmetry to be involved in delocalization with ***π***–electron systems of the organic ligands[4]. In the OMC systems, the electrons are free to move, which would create high nonlinearity from the interaction between laser light and the free electrons within the molecular structure of OMC systems[4]. Therefore, the physical origin of the nonlinear optical (NLO) properties of similar systems was reported by different research groups [5-9]. Also, the influence of the central metal atom on the nonlinear optical properties of metallophthalocyanines was investigated[10].

The thermal lens (TL) technique is considered as a very sensitive tool for investigating a large number of molecules in order to study their thermo-Physics, quantum yield, and NLO properties [11-13]. So, it was reported that the TL technique has been utilized to study the NLO properties of different molecules such as biomedical molecules [14, 15]. Fluorescein–Rhodamine B dye mixtures [16], sodium carbide nanoparticle [17], liquid ethanol, [18] series of primary alcohols [19, 20], multi-walled carbon nanotubes [21], carbon fiber [22], and organic-inorganic hybrid mixture [23].

In this article, the TL properties of the TCPC were investigated using the mode match dual-beam z-scan technique. Then, a new theoretical thermal lens model was implemented to achieve the best fit of the experimental data in order to extract the thermal lens parameters of this new TCPC complex, such as the convective velocity (v_x), the thermal diffusivity (D), the thermo-optic coefficient (dn/dT), the on-axis phase shift (θ), the thermal diffusion time (t_c), and the Peclet number (PE). The presence of a high NLO response in this kind of organic and inorganic system would help to create a deeper understanding of the behaviors of the TCPC, as well as provide a way to fabricate new optical modulators for future photonic applications. Therefore, we can describe the novelty of this research using a new complex molecule (TCPC), which consists of organic and inorganic components, representing a new alternative molecular system that gives a strong indication to use such a chromium complex in the field of optical modulator applications [24, 25].

2. Experimental techniques

The TCPC complex was already prepared and fully characterized using different spectroscopic techniques. The characterized data included the UV-Vis absorption and FTIR spectra of the TCPC complex; all details were mentioned in our previous work. [26]. Fig. 1 presents the molecular structure of the TCPC complex. The experimental setup of TL phenomena is based on the dual-beam mode-matched z-scan technique (Fig. 2). It is similar to the experimental setup used in our recently published works [27]. Here, we present some key parameters related to the experimental procedures. A diode green laser with a Gaussian beam (λ =532 nm) was used to excite the TCPC molecules. The green laser beam was focused into the 2 mm quartz cell using a positive lens with a focal point of 10 cm in a mode-matched configuration. Accordingly, the

absorption of incoming photons from the green laser will cause local sample heating, followed by the formation of a refractive index gradient, which produces a negative lens (TL). Then, for characterization of the formed lens, a low-power He-Ne laser beam (λ =632.8 nm) was sent to probe the thermal lens zone by recording the transmittance signals of He-Ne laser intensity changes, which depend on the nature of the thermal lens. The TL transmittance signals (the normalized intensity I/I_0) were taken as a function of time (t) with input pump powers (Pe = 3, 5, 10, and 15 mW). Later in the next step, a diode red laser beam with λ =635 nm replaced the green laser beam (λ =532 nm); it was used as a pump laser with the same low power He-Ne laser beam as a probe beam. The TCPC complex was dissolved in chloroform solvent with a concentration of 10^{-3} M. Both of the TL transmitted signals (pump and probe beams) were detected by two silicon photo-detectors (PD), which were connected to a Tektronix digital oscilloscope for tracing the TL effect signals of the TCPC solution. The 2 mm quartz cell used was fixed on a three-dimensional translational stage, and it moved along the z-axis through the focal point (z=0) by a control unit. All the experimental components were controlled by computer programs. The 2 mm quartz cell filled with TCPC solution was closed by a stopper in order to prevent evaporation of the solvent during the experimental data acquisition. A pulses generator was utilized to fire the pump laser beam in order to control the operating mode of the pump laser. This will allow for suitable modulation of the beam frequency and the selection of the full pump on/off cycle time.

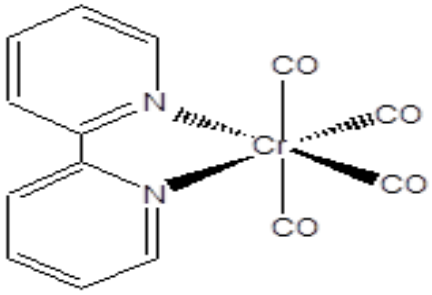

Fig. 1. Molecular structure of TCPC

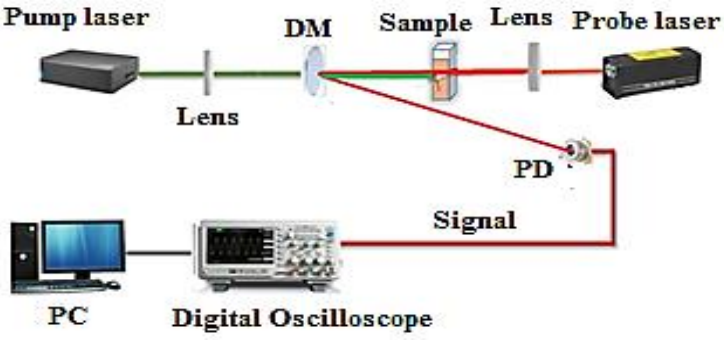

Fig. 2. The setup arrangements of dual-beam z-scan technique (color online)

Finally, it is useful to clarify some points about the typical single beam z-scan, which is a similar technique to the mode-matched dual-beam z-scan technique (explained above). The single beam z-scan usually utilizes a single laser beam for exciting the NL medium. It is employed to evaluate the NLO features of the studied sample molecules by recording the open and closed curves in order to calculate the nonlinear absorption coefficient (β) and the nonlinear refractive index (n_2) [24].

3. Results and discussion

In order to observe the time-resolved TL transient signals, a pulses generator was used to control the on/off exposure time of the pump laser beam onto the studied molecules. First, we recorded the TL variation signals as a function of time using a green pump laser beam (λe =532 nm) at different pump laser powers (Pe =3, 5, 10, 15 mW). Fig. 3 shows the observed TL variation signals (the normalized intensity I/I_0) as a function of time. The mean features of the recorded TL signals decrease with increasing laser excitation powers [28], and decreasing the values of t_c, which are consistent with the reported work in the literature [19, 27].

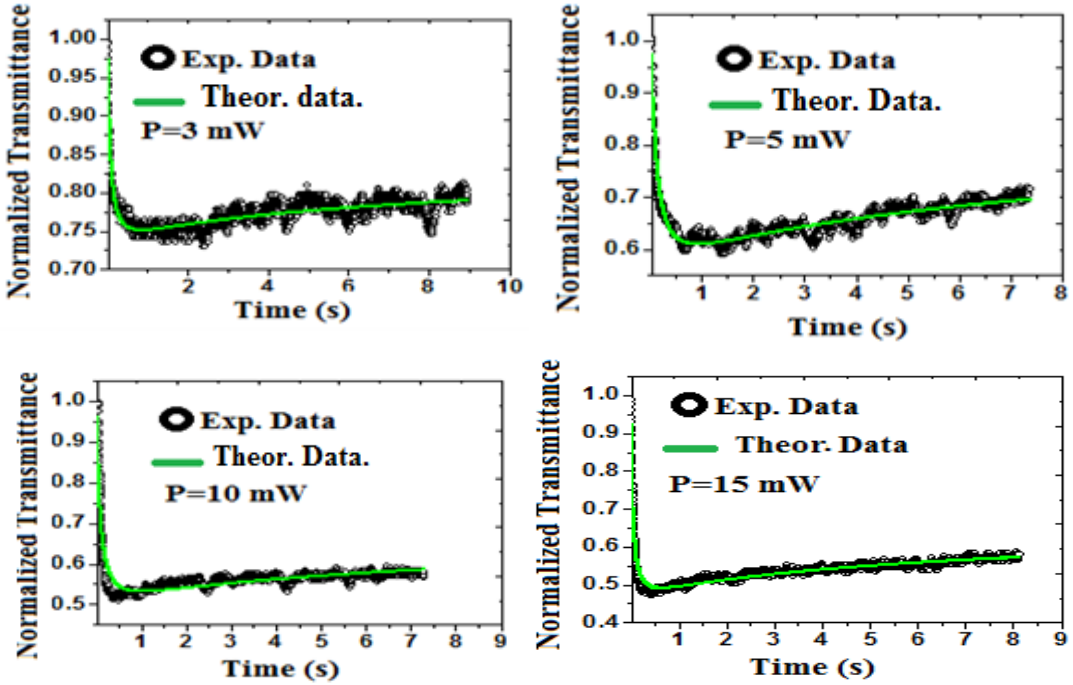

Fig. 3. Thermal lens effect induced by green laser beam (λe=532nm) in tetracarbonyl(2,2'-bipyridyl)chromium(0) complex sample, at laser powers of 3, 5, 10 and 15 mW (color online)

Using the numerical integration of the TL signal equation 1 to perform fitting of the experimental data [11], which includes the conductive and convective modes of heat transfer. The normalized TL signals can be measured using I(t)/I(0), where I(t) and I(0) are the probe laser intensity at the detector at the time t when t = 0. The intensity I(t) is the probe beam intensity when the excitation beam is on, and the intensity I(0) is considered the probe beam intensity when the excitation beam is off. S(t) can be defined as the time-resolved signal (equation 1) [11]:

$$S(t) = \frac{I(t)}{I(0)} = \left[1 - \frac{i\theta}{4}\left[-\left(\frac{P_E^2}{2} \times \frac{(1+iV-2m)^2}{2m(1+V)}\right)\left\{2i\tan^{-1}\left\{\frac{2mV}{\left[(1+2m)^2\right)+V^2\right]\left(\frac{t_c}{2t}\right)+1+2m+v^2}\right\}+\ln\left\{\frac{\left[1+\frac{2m}{\left(1+\frac{2t}{t_c}\right)}\right]^2+V^2}{(1+2m)^2+V^2}\right\}\right\} - P_E^2\left[\frac{2m}{(1+iV)}\ln\left(1+\frac{2t}{t_c}\right)+\left(\frac{\frac{2t}{t_c}}{1+\frac{2t}{t_c}}\right)\right]\right]\right]^2 \quad (1)$$

The parameters in equation 1 are defined as: $m = \left(\frac{\omega_p}{\omega_e}\right)^2$, where ωp and ωe are the beam waists of the probe and the pump beams at the sample position and $v = \left(\frac{z}{z_p}\right)$, where z is the distance of the sample from the beam waist position of probe beam and z_p is Rayleigh range of probe beam.

The Péclet number, PE

$$P_E = \frac{rate\ \ of\ \ convection}{rate\ \ of\ \ conduction} = \frac{\omega_e v_x}{4D} \quad (2)$$

And the on-axis phase shift θ:

$$\theta = \frac{\alpha P_e L}{k \lambda_p}\left(\frac{d n}{d T}\right) \quad (3)$$

where pe is the pump laser power, λp is the wavelength of the probe beam, α0 is the linear absorption coefficient, L is the sample thickness, dn/dT is the thermo-optic coefficient, and k is the thermal conductivity of the solvent.

The thermal diffusion time:

$$t_c = (\frac{\omega_e^{\ 2}}{4D}) \quad (4)$$

where D is the thermal diffusivity.

Solving equation 1 was performed with the help of the Matlab software. So, the experimental normalized TL signals of S(t) and the geometrical experimental parameters (m and V) were inserted into equation 1 in order to achieve the best fitting of the thermal lens curves. Then, we can extract from the best fitting processes the values of the Peclet number (PE), the thermal diffusion time t_c, and the on-axis phase shift (θ).

The solid lines in Fig. 3 are the results of the best fitting of the experimental data (circles) using equation 1[11]. Since, the generated solid lines pass through the experimental transient curves (Fig. 3) without any irregular features, it can be said that there is a good agreement between the experimental transient curves and the theoretical solid lines (TL model, equation 1). This means the theoretical TL model is applicable to the reported experimental results. Also, it was found that the TCPC complex acts as a self-defocusing medium (the TCPC solution behaves as a negative TL) due to a negative value of the thermo-optical coefficient (dn/dT). The value and the sign of the dn/dT can be calculated by recording the closed aperture z-scan of the TCPC solution, and the shape of the curve is like a peak-valley configuration. The calculation was performed in similar steps to our previous work[26]. The on-axis phase shift (θ) can be extracted from the best fitting process of equation 1. In addition, the value of (dn/dT) can be calculated using the z-scan experiment; then the value of θ can be determined using equation 3.

The formed negative thermal lens causes a decrease in the transmitted intensity of the probe laser beam. The transient TL signals indicate that the transmitted laser intensity would increase with time until reaching the final steady state. The rate of reduction of TL signals depends on the rate of the convection heat component[11]. It is important to compare the influence of convection on the TL signals when using the TCPC as a sample study. The output results of the applied theoretical model (equation 1) give the ratio of the convective heat transfer rate to the conductive heat transfer rate; this ratio is called the Péclet number (PE). Also, two fixed experimental parameters of m and V were calculated (m = 43.5 and V = 3.68) in order to be used later in the data fitting. The obtained fitting parameters dn/dT, D, v_x, t_c, PE, and θ are given in Table 1: the values of t_c and PE have decreased with increasing input laser powers, while θ has increased with increasing input laser powers.

Table 1. Summarizes the calculated thermal lens parameters of tc, PE , vx, D, dn/dT and θ, using the green pump laser with λe =532 nm, (m=43. 5 and V=3.68 at experimental configurations)

Power (mW)	t_c (s) $\times10^{-2}$	PE	θ	v_x(cm/s) $\times10^{-2}$	D(cm^2/s) $\times10^{-4}$	dn/dT (K^{-1})$\times10^{-3}$
3	**1.2**	**0.170**	**0.27**	**8.08**	**6.77**	**1.71**
5	**1.1**	**0.165**	**0.46**	**8.55**	**7.38**	**1.74**
10	**1**	**0.160**	**0.53**	**9.12**	**8.12**	**1.00**
15	**0. 5**	**0.150**	**0.58**	**17.1**	**16.20**	**0.73**

The results in Table 1 give an indication that the values of the Peclet number (PE) decreased with increasing input laser power; this fact can be explained [11], On the basis of the values of the Péclet number (PE), when PE >1, this indicates that the convection mode is the dominant mode of heat transfer compared to conduction. However, in our sample, all the values of PE are less than 1 (PE<1), which means that the conduction mode is the dominant factor of heat transfer compared to convection in our sample (the TCPC complex).

As the thermal lens will be formed as a result of heat generated in the local region of absorption, the refractive index will be modified and lead to a negative lens (divergent lens) in the TCPC complex, which means the sign of dn/dT is negative. To measure the amount of changes in the NL refractive index (n_2), which induces a phase shift proportional to the phase shift difference of the probe beam, θ, we have replaced the green pump laser (λe=532 nm) with a red pump laser (λe=635 nm) while keeping the same pump power lasers (Pe =3, 5, 10, and 15 mW). Fig. 4 presents the time dependence of normalized TL signals of the TCPC complex dissolved in chloroform with a concentration of 10^{-3}M (λ =635 nm) at different input pump powers.

The mean features of the recorded signals are (1) thermal lens signals decreased with increasing laser excitation energy [28], and (2) decreasing the time (t_c); these results are consistent with the reported work in the literature [19, 27]. Also, equation 1 was used to fit the experimental data [11]. The results of calculating parameters dn/dT, D, v_x, t_c, PE and θ using the fitting processes are given in Table 2.

Table 2. Summarizes the calculated thermal lens of t_c, PE, v_x, D, dn/dT and θ, using red pump laser with λ_e=635nm, (m=149 and V=3.68 at experimental configurations)

Power (mW)	t_c (s) $\times 10^{-2}$	PE	θ	v_x(cm/s) $\times 10^{-3}$	D(cm^2/s) $\times 10^{-5}$	dn/dT (K^{-1})$\times 10^{-4}$
3	**24**	**0.12**	**0.02**	**2.85**	**3.38**	**1.80**
5	**19**	**0.097**	**0.04**	**2.91**	**4.28**	**2.15**
10	**16.8**	**0.096**	**0.08**	**3.26**	**4.83**	**2.16**
15	**14.2**	**0.113**	**0.122**	**4.54**	**5.72**	**2.19**

Also, the fixed experimental parameters are m = 149 and V = 3.68. The t_c and PE have decreased with increasing input laser power, while the values of θ have increased with increasing input laser power. The differences between the results in Tables 1 and 2 are due to the absorption coefficients of the TCPC complex at the green pump laser wavelength (α_0 = 2.15 cm^{-1}) and the red pump laser wavelength (α_0 = 1.51 cm^{-1}).

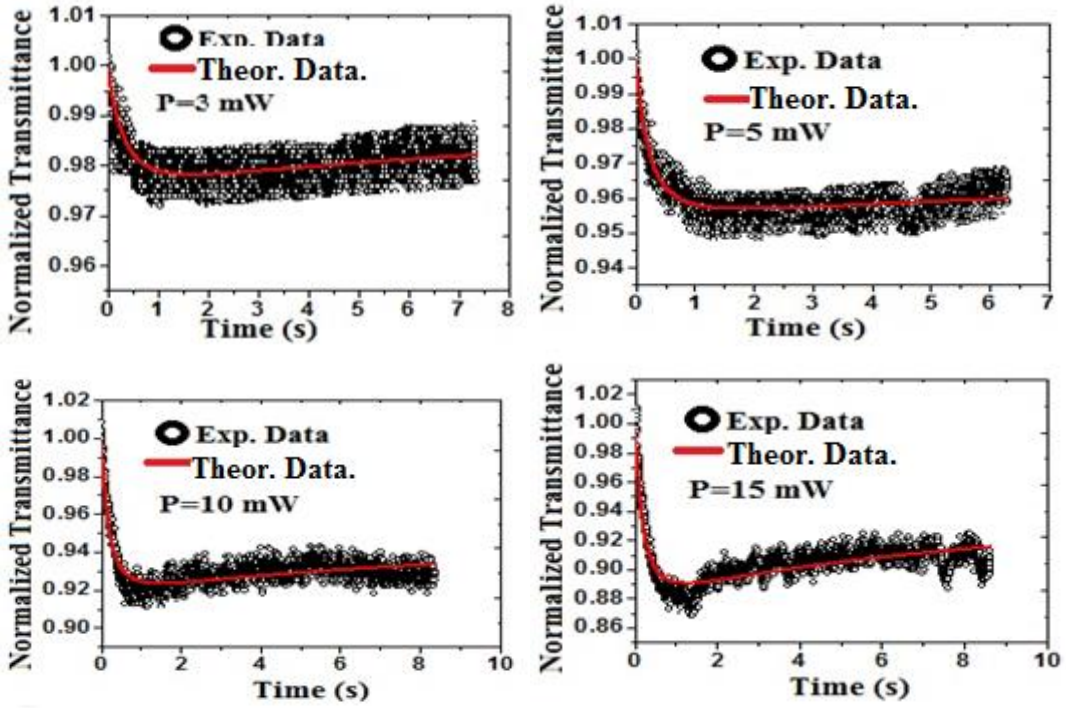

Fig. 4. Thermal lens effect induced by red laser beam (λe=635 nm) in tetracarbonyl (2,2'-ipyridyl) chromium(0) complex, at laser powers of 3, 5, 10 and 15 mW (color online)

The results show a strong absorption inside the sample when using the green laser beam (λ =532 nm) due to the resonant absorption region of the TCPC complex. This strong electronic resonance can make an enhancement to the optical nonlinearity in the TCPC complex[10].

Regarding the comparison between these results and other research, we think our present results agree with similar work reported in ref. [19, 20].

The uncertainties in Tables 1 and 2, the θ, v_x, PE, dn/dT, and tc arise from the measurement of the focal spot size (±5%), linear refractive index (±0.3%), linear absorption coefficient (±5%), and Rayleigh length (±4%). The maximum error in such measurements should be less than 5% for each parameter.

4. Conclusion

We have employed a pump-probe mode-matched TL configuration for measuring the thermal lens coefficients of TCPC. The observed TL signals decrease linearly with the laser pump powers. Two laser wavelengths were used as laser pumps in order to compare the TL signals; it was found that there is strong absorption inside the TCPC solution when using the green laser wavelength. This strong electronic absorption enhances the optical nonlinearity in the TCPC complex, which has led to a rise in the TL effect. We have implemented the theoretical TL model that includes the convective mode of heat dissipation to study the TL effects in the TCPC solution. The contribution of convective heat transfer in the TL effect is quantified in terms of the Péclet number (PE).

The TCPC can be promising candidates for a variety of optoelectronic/photonic applications.

Acknowledgements

We would like to thank the AEC of Syria for the financial support. Also, our thanks go to Prof. I. Othman, the head of AECS, and Prof. M. K. Sabra for their valuable help and discussion.

References

[1] A. Gerlach, T. Hosokai, S. Duhm, S. Kera, O. T. Hofmann, E. Zojer, J. Zegenhagen, F. Schreiber, Physical Review Letters **106**, 156102 (2011).
[2] A. Zawadzka, K. Waszkowska, A. Karakas, P. Płóciennik, A. Korcala, K. Wisniewski, M. Karakaya, B. Sahraoui, Dyes and Pigments **157**, 151 (2018).
[3] K. B. Manjunatha, R. Rajarao, G. Umesh, B. Ramachandra Bhat, P. Poornesh, Optical Materials **72**, 513 (2017).
[4] T. Huang, Z. Hao, H. Gong, Z. Liu, S. Xiao, S. Li, Y. Zhai, S. You, Q. Wang, J. Qin, Chemical Physics Letters **451**, 213 (2008).
[5] I. Fuks-Janczarek, I.V. Kityk, J. Berdowski, B. Sahraoui, C. Andraud, Journal of Modern Optics **52**, 1933 (2005).
[6] K. Iliopoulos, R. Czaplicki, H. El Ouazzani, J. Y. Balandier, M. Chas, S. Goeb, M. Sallé, D. Gindre, B. Sahraoui, Applied Physics Letters **97**, 10 (2010).
[7] M. Shoraka, M. R. Roknabadi, N. Shahtahmassebi, S. Sharifi, Optical and Quantum Electronics **56**, 955 (2024).
[8] F. A. Zarif Mahdizadeh, A. A. Esmaeili, Z. Zeraatkar, M. Behrouz, Z. Dehghani, L. A. Miccio, S. Sharifi, Optical and Quantum Electronics **55**(9), 6 (2023).
[9] M. Amirkhani, S. Sharifi, O. Marti, Journal of Physics D: Applied Physics **45**, 365302 (2012).
[10] B. Derkowska, M. Wojdyła, R. Czaplicki, W. Bała, B. Sahraoui, Optics Communications **274**, 206 (2007).
[11] S. Singhal, D. Goswami, Analyst **145**, 929 (2020).
[12] E. Dy, C. Gu, J. Shen, W. Qu, Z. Xie, X. Wang, M. L. Baesso, N. G. C. Astrath, Journal of Applied Physics **131**(6), 063102 (2022).
[13] M. Liu, Thermochimica Acta **672**, 126 (2019).
[14] G. Mazza, T. Posnicek, L.-M. Wagner, J. Ettenauer, K. Zuser, M. Gusenbauer, M. Brandl, Sensors and Actuators B: Chemical **249**, 731 (2017).
[15] E. Cedeño, H. Cabrera, A. E. Delgadillo-López, O. Delgado-Vasallo, A. M. Mansanares, A. Calderón, E. Marín, Talanta **170**, 260 (2017).
[16] A. Kurian, S. D. George, V. P. N. Nampoori, C. P. G. Vallabhan, Spectrochimica Acta Part A: Molecular and Biomolecular Spectroscopy **61**, 2799 (2005).
[17] M. S. Swapna, S. Sankararaman, International Journal of Thermophysics **41**, 93 (2020).
[18] M. H. Mahdieh, M. A. Jafarabadi, E. Ahmadinejad, XX International Symposium on High Power Laser Systems and Applications 2014, Proc. SPIE **9255**, 925531 (2015).
[19] S. Singhal, D. Goswami, ACS Omega **4**, 1889 (2019).
[20] P. Kumar, A. Khan, D. Goswami, Chemical Physics **441**, 5 (2014).
[21] Y. Guo, K. Ruan, X. Yang, T. Ma, J. Kong, N. Wu, J. Zhang, J. Gu, Z. Guo, Journal of Materials Chemistry C **7**, 7035 (2019).
[22] W. Si, J. Sun, X. He, Y. Huang, J. Zhuang, J. Zhang, V. Murugadoss, J. Fan, D. Wu, Z. Guo, Journal of Materials Chemistry C **8**, 3463 (2020).
[23] G. Argüello-Sarmiento, M. Ortiz-Gutiérrez, M. Trejo-Durán, J. A. Andrade-Lucio, J. E. Castellanos-Águila, E. Alvarado-Méndez, Journal of Molecular Liquids **383**, 122058 (2023).
[24] R. Abazari, E. Yazdani, M. Nadafan, A. M. Kirillov, J. Gao, A. M. Z. Slawin, C. L. Carpenter-Warren, Inorganic Chemistry **60**, 9700 (2021).
[25] Y. Hu, R. Abazari, S. Sanati, M. Nadafan, C. L. Carpenter-Warren, A. M. Z. Slawin, Y. Zhou, A. M. Kirillov, ACS Applied Materials and Interfaces **15**, 37300 (2023).
[26] M. D. Zidan , M. M. Al-Ktaifani, A. Allahham, Journal of Optoelectronics and Advanced Materials **20**(5-6), 314 (2018).
[27] M. D. Zidan, A. Arfan, M. S. EL-Daher, A. Allahham, A. Ghanem, D. Naima, Optical Materials **117**, 111133 (2021).
[28] M. R. Mohebbifar, Measurement **156**, 107611 (2020).

*Corresponding author: PScientific8@aec.org.sy